

**THERMAL AND OPTICAL PERFORMANCE OF  
InGaAlP-BASED LOW- AND GaN-BASED HIGH-  
POWER LIGHT-EMITTING DIODE PACKAGES**

**MUNA EZZI ABDULLAH RAYPAH**

**UNIVERSITI SAINS MALAYSIA**

**2020**

**THERMAL AND OPTICAL PERFORMANCE OF  
InGaAlP-BASED LOW- AND GaN-BASED HIGH-  
POWER LIGHT-EMITTING DIODE PACKAGES**

by

**MUNA EZZI ABDULLAH RAYPAH**

**Thesis submitted in fulfilment of the requirements  
for the degree of  
Doctor of Philosophy**

**February 2020**

## **ACKNOWLEDGEMENT**

First and foremost, all praise is to Allah S.W.T the Almighty, who gave me the patience, inspiration, and strength to fulfill this study.

I would like to express my most genuine gratitude to my main supervisor Associate Prof. Dr. Shahrom Mahmud for his valuable guidance and support. Indeed, his quick feedback and comments were helpful. I would also like to thank and express my sincere gratitude to my former main supervisor Associate Prof. Dr. Mutharasu Devarajan for his supervision and guidance during my PhD study. I am also grateful for his encouragement and support to create a good research environment.

I am fully thankful to Universiti Sains Malaysia (USM) for the financial support given by USM Fellowship from the Institute of Post-Graduate Studies (IPS) to carry out my PhD study. My appreciation and thanks go to the Faculty of Education in Hodeida University, Hodeida, Yemen for supporting me to pursue my PhD.

I would like to express deepest appreciation and thanks to my lab mates of Thermal Management Research Laboratory (TMRL), School of Physics, USM for the help provided during my study. I would also like to acknowledge the assistance of my fellow PhD lab mates for support and helping me in a technical discussion. My appreciation goes to Osram Opto Semiconductors and QAV Technologies Sdn. Bhd due to their support and allowing me to perform some experiments related to this research.

I am grateful to my family: my loving mother who supported and encouraged me to be confident whenever I faced the hardness and shouldered me in tough times, my father, my sisters, and my brothers.

**MUNA EZZI ABDULLAH**

## TABLE OF CONTENTS

<b>ACKNOWLEDGEMENT .....</b>	<b>ii</b>
<b>TABLE OF CONTENTS.....</b>	<b>iii</b>
<b>LIST OF TABLES .....</b>	<b>viii</b>
<b>LIST OF FIGURES .....</b>	<b>x</b>
<b>LIST OF SYMBOLS .....</b>	<b>xvii</b>
<b>LIST OF ABBREVIATIONS .....</b>	<b>xxi</b>
<b>ABSTRAK .....</b>	<b>xxiii</b>
<b>ABSTRACT .....</b>	<b>xxv</b>
<b>CHAPTER 1 INTRODUCTION .....</b>	<b>1</b>
1.1 Solid-State Lighting (SSL) Technology Challenges .....	1
1.2 Light-Emitting Diode Package.....	2
1.3 LED Thermal Management .....	3
1.4 Problem Statement .....	5
1.5 Objectives of Research .....	7
1.6 Thesis Outline .....	8
<b>CHAPTER 2 LITERATURE REVIEW.....</b>	<b>9</b>
2.1 Introduction.....	9
2.2 Conduction Heat Transfer Theory.....	9
2.3 Light-Emitting Diodes .....	12
2.4 LED Operation Principle .....	14
2.5 Overview on LED Packaging .....	16
2.5.1 Packaging of Low-Power LED .....	16
2.5.2 Packaging of High-Power LED.....	17
2.6 LED Thermal Characteristics.....	18
2.6.1 Heat Transfer Mechanism in LED Package.....	18

2.6.2	Thermal Measurements of LEDs.....	19
2.6.3	Structure Functions .....	20
2.6.4	Junction Temperature, $T_j$ .....	22
2.6.5	Thermal Resistance, $R_{th}$ .....	23
2.6.6	Thermal Time Constant, $\tau_{th}$ .....	24
2.7	LED Optical Characteristics .....	26
2.7.1	Luminous Flux, $\phi_v$ .....	26
2.7.2	Luminous Efficacy, $\eta_v$ .....	27
2.7.3	LED Emission Spectrum.....	27
2.7.4	Color .....	28
2.8	Package Level Thermal Management .....	29
2.8.1	Substrates .....	29
2.8.2	Thermally Conductive Materials (TCMs).....	30
2.8.3	Solders.....	32
2.8.4	Voids of Solder Layer.....	33
2.9	Instruments Description.....	35
2.9.1	Thermal Transient Tester (T3Ster) .....	35
2.9.1(a)	T3Ster Thermostat .....	36
2.9.1(b)	T3Ster Power Booster .....	37
2.9.1(c)	Evaluation of Heating/Cooling Curve.....	37
2.9.2	Thermal and Photometric/Radiometric Characterization of Power LEDs (TeraLED) .....	38
2.9.3	IR Imaging Camera (thermoIMAGER TIM 160, Micro-Epsilon®) .....	39
2.9.4	Spectrometer (CAS 140CT-Instrument System).....	39
2.10	Theoretical Background.....	40
2.10.1	Estimation of Heat-Dissipation Factor and Optical Power .....	40
2.10.2	Luminous Flux Analysis .....	42

2.10.3	Modeling Spectrum.....	44
2.11	Chapter Summary.....	49
<b>CHAPTER 3 METHODOLOGY AND EXPERIMENTAL PROCEDURES</b>		
.....		<b>50</b>
3.1	Introduction.....	50
3.2	Calibration Measurement of LEDs Under Test .....	51
3.3	Experiments on InGaAlP LP SMD LEDs .....	53
3.3.1	Effect of Substrate on Thermal and Optical Performance of InGaAlP LP SMD LED .....	53
3.3.1(a)	Description of Samples .....	53
3.3.1(b)	Thermal Transient Measurement.....	55
3.3.1(c)	Combination of Thermal and Optical Measurement .....	57
3.3.2	Influence of Thermal Interface Material on Performance of InGaAlP LP SMD LED .....	58
3.3.3	Measurement of Optical and Spectrum Characterizations of InGaAlP LP SMD LED .....	60
3.4	Experiments on ThinGaN HP SMD LEDs .....	61
3.4.1	Effects of Solder Type on Performance of ThinGaN HP SMD LED .....	61
3.4.1(a)	Description of Samples .....	62
3.4.1(b)	Description of Solders.....	63
3.4.1(c)	Measurement of Thermal and Optical Characterizations of ThinGaN HP LED with Different Solders .....	65
3.4.2	Effects of Solder Voids on Performance of ThinGaN HP SMD LED .....	66
3.4.2(a)	Description of Samples .....	66
3.4.2(b)	Measurement of Thermal and Optical Characterizations of ThinGaN HP SMD LED with Different Voids .....	67
3.4.3	Dynamic Thermal Analysis of ThinGaN HP SMD LEDs Using Multi-Exponential Function Model .....	68
3.5	Chapter Summary.....	70

<b>CHAPTER 4</b>	<b>THERMAL AND OPTICAL PERFORMANCE OF InGaAlP LP AND ThinGaN HP SMD LEDs .....</b>	<b>71</b>
4.1	Introduction.....	71
4.2	Thermal and Optical Performance of InGaAlP LP SMD LEDs .....	72
4.2.1	Variation of Thermal Resistance of InGaAlP LP SMD LED with Current and Temperature .....	72
4.2.2	Effect of Substrate Type on Performance of InGaAlP LP SMD LED .....	75
4.2.2(a)	Thermal Characterizations .....	75
4.2.2(b)	Optical Characterizations .....	80
4.2.3	Influence of Thermally Conductive Materials on Performance of InGaAlP LP SMD LED .....	85
4.2.4	Estimation of Heat-Dissipation Factor and Optical Power of InGaAlP LP SMD LED .....	96
4.2.4(a)	Test on Amber (LA E67F) LP SMD LED .....	96
4.2.4(b)	Test on Red (LR E67F) LP SMD LED.....	100
4.2.5	Luminous Flux Analysis of InGaAlP LP SMD LED .....	104
4.2.5(a)	Test on LED mounted on FR4 with 6.28 K/W.....	104
4.2.5(b)	Test on LED mounted on MCPCB with 3.14 K/W .....	107
4.2.5(c)	Test on LED mounted on MCPCB with 1.25 K/W .....	108
4.2.6	Modeling of Spectral Radiant Flux of InGaAlP LP SMD LED...	110
4.3	Thermal and Optical Performance of ThinGaN HP SMD LEDs.....	118
4.4	Effect of Solder Type on Performance of ThinGaN HP SMD LED.....	118
4.4.1(a)	Thermal Performance Analysis .....	119
4.4.1(b)	Optical Performance Analysis.....	126
4.5	Effects of Solder Voids on Performance of ThinGaN HP SMD LED.....	128
4.5.1(a)	Analysis of Thermal Performance .....	130
4.5.1(b)	Analysis of Optical Performance.....	135
4.5.2	Dynamic Thermal Analysis of ThinGaN HP SMD LED .....	139

4.6	Chapter Summary.....	152
<b>CHAPTER 5 CONCLUSION AND FUTURE RECOMMENDATIONS....</b>		<b>154</b>
5.1	Conclusion .....	154
5.2	Recommendations for Future Research.....	155
<b>REFERENCES .....</b>		<b>156</b>
<b>APPENDICES</b>		
<b>LIST OF PUBLICATIONS</b>		



## LIST OF TABLES

		<b>Page</b>
Table 3.1	Characteristics of LED under test at temperature 25 °C and current 50 mA [26, 184], materials data of substrate packages .....	54
Table 3.2	LED characteristics (at 700 mA and 25 °C) and maximum ratings along with data of SinkPAD MCPCB .....	63
Table 3.3	Specifications of lead-free solders (taken from solders datasheets) ..	64
Table 4.1	Thermal parameters of InGaAlP LED mounted on different substrates at 50 and 100 mA .....	80
Table 4.2	Parameters of InGaAlP LP SMD LED mounted on FR4 substrate...	88
Table 4.3	Parameters of InGaAlP LP SMD LED mounted on 2W MCPCB ....	90
Table 4.4	Parameters of InGaAlP LP SMD LED mounted on 5W MCPCB ....	92
Table 4.5	Wall-plug efficiency coefficients for amber LED.....	97
Table 4.6	Wall-plug efficiency coefficients for red LED.....	102
Table 4.7	Fitting parameters of junction temperature versus ambient temperature.....	112
Table 4.8	Fitting parameters of the spectrum model for the LEDs at 298 K ..	114
Table 4.9	Variation in carrier temperature, peak frequency, and energy gap together with characteristic temperature .....	115
Table 4.10	Comparison between practical and calculated luminous flux and CIE color coordinates of the LEDs at 348 K .....	117
Table 4.11	Voids% of the three solders on the LED thermal pad .....	119
Table 4.12	Voids% of the solder on the LED thermal pad for the samples .....	129
Table 4.13	Thermal resistance and temperature rise at 700 mA and 25 °C.....	132
Table 4.14	Mean (M) value and standard deviation (SD) of thermal time constant .....	143

Table 4.15	Temperature rise, thermal time constant, thermal resistance, and thermal capacitance of the LEDs' layers .....	145
Table 4.16	Chip size, package size together with material properties [136, 255-257] and thermal parameters of LEDs package substrate.....	147
Table 4.17	Comparison of thermal resistance and optical efficiency between LED manufacturer and this study .....	152

## LIST OF FIGURES

		<b>Page</b>
Figure 1.1	LED industry chain of manufacturing [3].....	1
Figure 1.2	LED-based lighting system levels .....	2
Figure 1.3	Typical lead frame LED package structure and parts functions [14] .....	3
Figure 2.1	Thermal conduction with energy diffusion due to molecular activities [44] and particle collisions .....	10
Figure 2.2	Thermal conduction by lattice vibrations [45] .....	10
Figure 2.3	One-dimensional thermal conduction analysis [47] .....	10
Figure 2.4	Process of photon emission in (a) direct bandgap and (b) indirect bandgap semiconductors [52].....	12
Figure 2.5	Schematic diagram of energy band for (a) homojunction LED and (b) double-heterostructure LED [53] .....	13
Figure 2.6	Schematic sketch of double-heterostructure LED and a battery for operating the LED [53] .....	15
Figure 2.7	An example of Osram LP SMD LED package (TOPLED) and its schematic diagram [64].....	16
Figure 2.8	HP LEDs with SMD packages: (a) LED chip attached to heat slug, (b) structure of Osram Dragon series LED, (c) LED chip attached to a ceramic substrate, and (d) structure of LUXEON Rebel of Philips Lumileds [69].....	18
Figure 2.9	Thermal transient measurement of LED package [21] .....	19
Figure 2.10	(a) Heating followed by cooling cycle [71] and (b) actual transient of a diode that scaled in voltage and temperature [21] .....	20
Figure 2.11	Practical comprehension of the diode measurement scheme at applying: (a) heating current and (b) measured current [21] .....	21

Figure 2.12	(a) Foster network and (b) Cauer network [76].....	21
Figure 2.13	Graphical representation of the calculation flow from measurement to the structure functions [156].....	38
Figure 3.1	Flow chart for design of experiment.....	50
Figure 3.2	Calibration curves of InGaAlP LP LED at different sensor current..	51
Figure 3.3	Calibration curves of ThinGaN HP LED at different sensor current .....	52
Figure 3.4	Optical image of cross-section view for InGaAlP LED together with zoom-in view .....	53
Figure 3.5	Schematic of InGaAlP LED internal structure [183] mounted on Al substrate: white arrows show the primary heat flow path through the lead frames to the end of leads by heat conduction and blue arrows indicate the heat convection .....	54
Figure 3.6	InGaAlP LED mounted on substrates (a) FR4 and (b) Al-based MCPCB .....	55
Figure 3.7	Calibration curves of InGaAlP SMD LED mounted on different substrates .....	56
Figure 3.8	Schematic of experiment setup for thermal transient measurement..	56
Figure 3.9	Combination of thermal and optical measurement setup (the DUT is inside the integrating sphere of TeraLED) .....	57
Figure 3.10	Schematic of experiment setup for optical and thermal measurements .....	58
Figure 3.11	Cross section of the LED package fixed on Al MCPCB .....	59
Figure 3.12	Schematic of the process of proposed embedding packaging structure.....	59
Figure 3.13	Measurement system of the LED spectrum .....	60
Figure 3.14	Schematic of the LED spectrum measurement setup .....	61
Figure 3.15	Optical image of cross-section view of ThinGaN HP LED.....	62

Figure 3.16	(a) ThinGaN HP LED package, (b) bottom surface view, and (c) LED package on SinkPAD MCPCB .....	62
Figure 3.17	ThinGaN LED package attached to SinkPAD using three solder types .....	64
Figure 3.18	(a) Microscopic image of the solder on SinkPAD pads and (b) LED package on SinkPAD .....	64
Figure 3.19	Reflow soldering profile of the three solders .....	65
Figure 3.20	Experiment setup for thermal imaging measurements .....	66
Figure 3.21	Cross-sectional view and heat flow path of (a) LED1 and LED3, and (b) LED2.....	68
Figure 3.22	Calibration curves of HP SMD LEDs under test.....	69
Figure 4.1	Differential structure functions of InGaAIP LED at different (a) input currents and (b) ambient temperatures.....	73
Figure 4.2	Junction temperature rise of InGaAIP LED at different (a) input currents and (b) ambient temperatures.....	74
Figure 4.3	Heat distribution in the substrate packages (a) FR4, (b) 2W MCPCB, and (c) 5W MCPCB [197] .....	75
Figure 4.4	Differential structure functions of InGaAIP LED mounted on different substrates at (a) 50 mA and (b) 100 mA: inset figure is zoom in on Region 1 .....	76
Figure 4.5	Cumulative structure functions of InGaAIP LED mounted on different substrates at (a) 50 mA and (b) 100 mA.....	77
Figure 4.6	Junction temperature rise of InGaAIP LED mounted on different substrates at (a) 50 mA and (b) 100 mA .....	79
Figure 4.7	Luminous efficacy of InGaAIP LED versus (a) input current and (b) ambient temperature .....	81
Figure 4.8	Wall-plug efficiency of InGaAIP LED versus (a) input current and (b) ambient temperature .....	82

Figure 4.9	Heat dissipation of InGaAlP LED versus (a) input current and (b) ambient temperature .....	83
Figure 4.10	Real thermal resistance of InGaAlP LED versus (a) input current and (b) ambient temperature .....	85
Figure 4.11	Schematic of thermal resistance model of (a) traditional structure and (b) proposed structure.....	86
Figure 4.12	Differential structure functions of InGaAlP LED on FR4 at 50 mA .....	87
Figure 4.13	Temperature rise of InGaAlP LED on FR4 substrate at 50 and 100 mA .....	88
Figure 4.14	Differential structure functions of InGaAlP LED mounted on 2W MCPCB at 50 mA.....	89
Figure 4.15	Temperature rise of InGaAlP LED on 2W MCPCB at 50 and 100 mA .....	90
Figure 4.16	Differential structure functions of InGaAlP LED mounted on 5W MCPCB at 50 mA.....	91
Figure 4.17	Temperature rise of InGaAlP LED on 5W MCPCB at 50 and 100 mA .....	92
Figure 4.18	Luminous flux as a function of electrical power of InGaAlP LP LED mounted on different substrates .....	94
Figure 4.19	Luminous flux as a function of electrical power due to the effect of substrate and TIM for InGaAlP LP LED mounted on (a) FR4, (b) 2W MCPCB, and (c) 5W MCPCB .....	95
Figure 4.20	Wall-plug efficiency of amber LP LED versus (a) electrical power and (b) ambient temperature .....	97
Figure 4.21	Wall-plug efficiency of amber LP LED as a 2D function of electrical power and ambient temperature .....	98
Figure 4.22	(a) Wall-plug efficiency, (b) heat-dissipation factor, and (c) optical power of amber LP LED versus electrical power .....	99

Figure 4.23	Wall-plug efficiency of red LP LED versus (a) electrical power and (b) ambient temperature .....	101
Figure 4.24	Wall-plug efficiency of red LP LED as a 2D function of electrical power and ambient temperature .....	102
Figure 4.25	(a) Wall-plug efficiency, (b) heat-dissipation factor, and (c) optical power of red LP LED versus electrical power .....	103
Figure 4.26	Luminous efficacy as a function of junction temperature for InGaAlP LP LED on FR4 .....	105
Figure 4.27	Junction to solder point thermal resistance and electrical power of InGaAlP LP LED on FR4 .....	105
Figure 4.28	Measured and calculated: (a) luminous flux and (b) efficacy of InGaAlP LP LED on FR4 with 6.28 K/W .....	106
Figure 4.29	Measured and calculated: (a) luminous flux and (b) efficacy of InGaAlP LP LED on MCPCB with 3.18 K/W.....	107
Figure 4.30	Measured and calculated: (a) luminous flux and (b) efficacy of InGaAlP LP LED on MCPCB with 1.25 K/W.....	108
Figure 4.31	Measured and calculated luminous flux curves of InGaAlP LP LED mounted on substrates with different thermal resistance at 25 °C.....	109
Figure 4.32	Effect of (a) input current and (b) ambient temperature on spectrum of LED A1 .....	111
Figure 4.33	Junction temperature as a function of ambient temperature .....	111
Figure 4.34	(a) Solid line is practical spectrum and dashed line is modeled spectrum at 298 K, (b) curve according to exponential fits, and (c) Gaussian fit curve .....	113
Figure 4.35	Peak frequency and ambient temperature for LEDs under test.....	115
Figure 4.36	Optical power variation with ambient temperature for LEDs under test.....	116
Figure 4.37	Comparison between experimental (solid lines) and calculated (dashed lines) spectra of A3 at different ambient temperatures .....	117

Figure 4.38	X-ray voids images for (a) SP1, (b) SP2, and (c) SP3.....	118
Figure 4.39	(a) Cumulative and (b) differential structure functions for ThinGaN LED with different solder pastes at 700 mA .....	120
Figure 4.40	Thermal resistance versus (a) input current at temperature 25 °C and (b) ambient temperature at current 700 mA .....	122
Figure 4.41	Junction temperature rise of the LEDs with different solders at 700 mA .....	123
Figure 4.42	Junction temperature rise versus (a) input current at temperature 25 °C and (b) ambient temperature at current 700 mA .....	123
Figure 4.43	Time-constant spectra of LEDs with different solders. Inset figure shows a magnification of the second peak.....	124
Figure 4.44	IR thermal images of temperature distribution at 700 mA for ThinGaN LED with (a) SP1, (b) SP2, and (c) SP3.....	125
Figure 4.45	Output power variation of the samples with input current and insets: thermal resistance and output power at 700 mA and magnification for the input current from 1100 to 1200 mA.....	126
Figure 4.46	(a) Chromaticity points in CIE 1931 chromaticity diagram, (b) color coordinates, and (c) color temperature of ThinGaN LED with different solders .....	127
Figure 4.47	X-ray images of the samples with different voids fraction .....	129
Figure 4.48	Cross-sectional view of voids at thermal pad together with magnification view .....	129
Figure 4.49	(a) Differential and (b) cumulative structure functions of the LEDs .....	130
Figure 4.50	Junction temperature rise of LEDs under test at 700 mA and 25 °C .....	132
Figure 4.51	Time-constant spectra of the LEDs under test at 700 mA and 25 °C: the inset is the magnification of the second peak.....	134
Figure 4.52	Thermal IR images of LED1 to LED5 (from (a) to (e)) at 700 mA	134



Figure 4.53	Luminous flux and efficacy with input current: inset figures (a) and (b) are the luminous flux and efficacy at current 1100 and 1200 mA, respectively.....	136
Figure 4.54	Relative spectral power distribution of the samples at 700 mA.....	136
Figure 4.55	(a) CIE 1931 chromaticity diagram, (b) chromaticity coordinates, and (c) CCT variation with current of the samples at 80 °C.....	138
Figure 4.56	Side view and dimensions of (a) LED1 and LED3, and (b) LED2 .	139
Figure 4.57	Spectra of the LEDs under test at different input currents and 25 °C .....	141
Figure 4.58	Junction temperature growth curves of LED2 at various (a) input currents and (b) ambient temperatures.....	142
Figure 4.59	Variation of thermal time constant of the LEDs with (a) input current and (b) ambient temperature.....	143
Figure 4.60	(a) Cooling transient curves at 700 mA and (b) LED1 cooling transient curve with three different layers.....	144
Figure 4.61	(a) Differential structure functions of LEDs and (b) structure functions of LED2 at 700 mA and 25 °C .....	148
Figure 4.62	Cumulative structure functions for (a) LED1 and (b) LED2 .....	150
Figure 4.63	Variation of junction temperature with input current for the LEDs	150
Figure 4.64	Time constant spectra of the LEDs under test at 700 mA and 25 °C .....	151

## LIST OF SYMBOLS

$T_a$	Ambient temperature [°C]
$B(\lambda)$	Asymmetrical line width [nm]
$E_g$	Band gap energy [eV]
$E_{g,ref}$	Band gap energy at reference temperature [eV]
$k$	Boltzmann constant = $8.617 \times 10^{-5}$ [eV/K]
$T_c$	Carrier temperature [K]
$T_{c,ref}$	Carrier temperature at reference temperature [K]
$\Delta V_f$	Change in forward voltage [V]
$T_{char}$	Characteristic temperature [K]
$x, y$	Chromaticity coordinates of CIE 1931 chromaticity diagram
$\Delta E$	Chromaticity deviation in CIE 1976 chromaticity diagram
$R^2$	Coefficient of determination
$\bar{x}(\lambda), \bar{y}(\lambda), \bar{z}(\lambda)$	Color matching functions of CIE 1931
$\Delta CCT$	Correlated color temperature deviation [K]
$A$	Cross-sectional area [m <sup>2</sup> ]
$C_{th\Sigma}$	Cumulative thermal capacitance [J/K]
$R_{th\Sigma}$	Cumulative thermal resistance [K/W]
$\rho$	Density [kg/m <sup>3</sup> ]
$I_D$	Drive current [A]
$P_{el}$	Electrical input power [W]
$R_{th,el}$	Electrical thermal resistance [K/W]
$I_f$	Forward or input current [A]
$V_f$	Forward voltage [V]
$\nu$	Frequency [Hz]
$\nu_G$	Gaussian peak frequency [Hz]

$P_{heat}$	Heat dissipation power [W]
$q_x''$	Heat flux [W/m <sup>2</sup> ]
$q_x$	Heat transfer rate [J/s]
$k_h$	Heat-dissipation factor [%]
$I_H$	Heating current [A]
$T_j$	Junction temperature [°C]
$\Delta T_j$	Junction temperature rise [°C]
$V_{fpn}$	Junction voltage [V]
K	K-Factor [K/mV]
$d$	Length [m]
$S_1^{-1}, S_2^{-1}$	Low and high energy tail of the spectrum [W]
$\eta_v$	Luminous efficacy [lm/W]
$\eta_{vo}$	Luminous efficacy at 25 °C [lm/W]
$V(\lambda)$	Luminous efficiency function
$\varphi_v$	Luminous flux [lm]
$I_M$	Measured current [A]
$P_{opt}$	Optical output power [W]
$\nu_p$	Peak frequency [Hz]
$\nu_{p,ref}$	Peak frequency at reference temperature [Hz]
$\lambda_p$	Peak wavelength [nm]
h	Planck constant = 4.136 x 10 <sup>-15</sup> [eV.s]
$\propto$	Proportionality symbol
$R_{th,real}$	Real thermal resistance [K/W]
$T_{ref}$	Reference temperature [°C]
$\Delta R_{thja-TCA}$	Relative change in $R_{thja}$ due to TCA
$\Delta R_{thja-TCE}$	Relative change in $R_{thja}$ due to TCE
$\Delta R_{thjs-TCA}$	Relative change in $R_{thjs}$ due to TCA

$\Delta R_{thjs-TCE}$	Relative change in $R_{thjs}$ due to TCE
$\Delta R_{thja-2W}$	Relative increase in $R_{thja}$ between 2W and 5W MCPCB
$\Delta R_{thja-FR4}$	Relative increase in $R_{thja}$ between FR4 and 5W MCPCB
$\Delta R_{thjs-2W}$	Relative increase in $R_{thjs}$ between 2W and 5W MCPCB
$\Delta R_{thjs-FR4}$	Relative increase in $R_{thjs}$ between FR4 and 5W MCPCB
I	Relative intensity of radiation
$k_e$	Relative reduction rate of efficacy [ $K^{-1}$ ]
$I_S$	Sensor current [A]
$R_S$	Series resistance [Ohm]
$S_3$	Single color spectrum peak value [W]
$\delta$	Slope of carrier temperature variation with temperature
$\omega_p$	Slope of peak frequency variation with temperature [Hz/K]
$k_{js}$	Slope of thermal resistance vs electrical power [ $K/W^2$ ]
$c_{th}$	Specific heat [J/kg. K]
$S_0$	Spectral intensity at the peak wavelength [W/nm]
$\Phi_\lambda, \Phi_\nu$	Spectral radiant flux [W/nm] or [W/Hz]
c	Speed of light (in vacuum) = 299792458 [m/s]
$dT/dx$	Temperature gradient along x-direction [K/m]
$k_{th}$	Thermal conductivity [W/m.K]
$R_{th}$	Thermal resistance [K/W]
$R_{thja}$	Thermal resistance from junction to ambience [K/W]
$R_{thjs}$	Thermal resistance from junction to solder point [K/W]
$R_{th,P}$	Thermal resistance of proposed structure
$R_{th,solder}$	Thermal resistance of solder layer
$R_{th,TIM}$	Thermal resistance of TIM [K/W]
$\tau_{th}$	Thermal time constant [s]
t	Time [s]

$\alpha_V, \beta_V$	Varshni parameters [meV/K], [K]
$c_V$	Volumetric heat capacitance [J/m <sup>3</sup> .K]
$\eta_w$	Wall-plug efficiency or optical efficiency [%]
$\lambda$	Wavelength [nm]

## LIST OF ABBREVIATIONS

1D and 2D	One- and two-dimensional
Al	Aluminum
Al <sub>2</sub> O <sub>3</sub>	Aluminum oxide
AlN	Aluminum nitride
CB	Conduction band
CCT	Correlated color temperature
CIE	International Commission on Illumination
CIE <sub>x</sub> , CIE <sub>y</sub>	CIE chromaticity coordinates
CRI	Color rendering index
CTE	Coefficient of thermal expansion
Cu	Copper
DAA	Die attach adhesive
DH	Double heterostructure
DUT	Device under test
EDX	Electron Dispersion X-Ray
EL	Electroluminescence
EQE	External quantum efficiency
FESEM	Field-Emission Scanning Electron Microscope
FR4	Flame retardant fibre glass epoxy
GaAs	Gallium arsenide
GaN	Gallium nitride
Ge	Germanium
HP	High power
IMS	Insulated metal substrate
InGaAlP	Indium gallium aluminum phosphide
IPC	Institute for Printed Circuits
IR	Infrared
JEDEC	Joint Electron Device Engineering Council
LCD	Liquid crystal display
LED	Light-emitting diode
LP	Low power

MCPCB	Metal core printed circuit board
MQW	Multi quantum well
NID	Network identification by deconvolution
pc	Phosphor-converted
PCB	Printed circuit board
RGB	Red green blue
SAC	Tin silver copper
SD	Standard deviation
Si	Silicon
SMD	Surface-mounted device
SP	Solder paste
SPD	Spectral power distribution
SSL	Solid-state lighting
T3Ster	Thermal transient tester
TCA	Thermally conductive adhesive
TCE	Thermally conductive epoxy
TCM	Thermally conductive material
TeraLED	Thermal and radiometric characterization of LEDs
TIM	Thermal interface material
TSP	Temperature sensitive parameter
UV	Ultraviolet
VB	Valence band
WPE	Wall-plug efficiency
YAG	Yttrium aluminum garnet

**PRESTASI TERMA DAN OPTIK PAKEJ DIOD PEMANCAR CAHAYA  
BERASASKAN InGaAlP BERKUASA RENDAH DAN GaN BERKUASA  
TINGGI**

**ABSTRAK**

Diod pemancar cahaya (LED) dengan peranti yang dipasang di permukaan (SMD) telah digunakan dalam aplikasi pencahayaan. Salah satu masalah utama dalam teknologi pencahayaan ialah pengurusan haba peranti. Kajian ini dibahagikan kepada tiga bahagian utama. Pada bahagian pertama, prestasi indium gallium aluminium fosfida (InGaAlP) SMD LED kuasa rendah (LP) dilekatkan ke substrat dengan konfigurasi yang berlainan. LED telah dilekatkan pada substrat FR4 dan papan litar bercetak logam teras berasaskan aluminium (MCPCBs) dengan kekonduksian terma yang berbeza. Telah didapati bahawa jumlah rintangan haba ( $R_{thja}$ ) adalah masing-masing 95.3, 66.4, dan 60.7 K / W untuk LED pada FR4 dan MCPCBs. Kecekapan optik ( $\eta_w$ ) ialah 40.2%, 41.1%, dan 42.0%. Di samping itu, prestasi LED menggunakan epoksi konduktif termal (TCE) dan pelekat (TCA) dilekatkan di antara pakej dan substrat LED juga telah disiasat. Telah diperhatikan bahawa LED pada FR4 dan MCPCB dengan TCA mempunyai  $R_{thja}$  sebanyak 66.1, 51.2, 50.5 K / W, masing-masing dan  $\eta_w$  adalah 58.6%, 54.1%, dan 52.7%. Pada bahagian kedua kajian, faktor pelepasan haba, kuasa optik, fluks bercahaya dan fluks spektrum LED LP dianggarkan dengan memperluaskan penggunaan persamaan yang digunakan untuk LED berkuasa tinggi (HP). Telah didapati terdapat ralat relatif kurang daripada 15% antara nilai kiraan dan nilai praktikal. Pada bahagian ketiga kajian, prestasi HP LED gallium nitride nipis (ThinGaN) yang dipasang pada SinkPAD melalui solder telah diselidik. Tiga jenis pateri: SAC305 yang tidak di bersih (SP1), SAC305 yang boleh dibasuh



dengan air (SP2), dan Sn42 / Bi57.6 / Ag0.4 yang tidak bersih (SP3) telah digunakan. Penemuan mendedahkan bahawa  $R_{thja}$  untuk SP1, SP2, dan SP3 adalah 5.76, 6.09, dan 6.65 K / W. Dengan cara yang sama, pada 1200 mA, kuasa output masing-masing adalah 1330, 1288, dan 1279 mW. Selain itu, bagi julat semasa 400-1200 mA, peralihan suhu warna (CCT) berkorelasi ialah 350, 406, dan 768 K. Kesan lompong udara SP2 pada prestasi LED dinilai. Analisis menunjukkan bahawa  $R_{thja}$  adalah 6.29, 5.79, 6.09, 6.39, dan 7.71 K / W untuk LED 1-5. Tambahan pula, pada 1200 mA dan 80 °C, fluks bercahaya ialah 371.5, 367.8, 373.0, 360.3, dan 351.7 lm. Selain itu, bagi julat semasa 400-1200 mA, perubahan dalam CCT adalah 755, 831, 1046.5, 1019, dan 1779 K untuk LED dari 1 hingga 5. Selain itu, prestasi dinamik terma LED telah dianalisis dengan menggunakan fungsi pelbagai eksponen model. Telah ditunjukkan bahawa pemalar masa pakej LED adalah pada urutan 22 hingga 94 ms.

**THERMAL AND OPTICAL PERFORMANCE OF InGaAlP-BASED  
LOW- AND GaN-BASED HIGH-POWER LIGHT-EMITTING DIODE  
PACKAGES**

**ABSTRACT**

Surface-mounted device (SMD) light-emitting diodes (LEDs) have been employed in state-of-the-art illumination applications. One of the major bottlenecks in lighting technology is the device heat management. This study was divided into three main parts. In the first part, the performance of indium gallium aluminum phosphide (InGaAlP) low-power (LP) SMD LED affixed to substrates with different configurations. The LED was attached to substrates which were Flame Retardant 4 printed circuit board (FR4 PCB) and aluminum-based metal core PCB (MCPCBs) with different thermal conductivity (2 and 5 W/m.K). It was found that the total thermal resistance ( $R_{thja}$ ) was 95.3, 66.4, and 60.7 K/W for the LEDs on FR4 and MCPCBs, respectively. Similarly, the optical efficiency ( $\eta_w$ ) was 40.2%, 41.1%, and 42.0%. Additionally, the LED performance using thermally conductive epoxy (TCE) and adhesive (TCA) embedded between the LED package and substrate was investigated. It was observed that the LED on the FR4 and MCPCBs with TCA has  $R_{thja}$  of 66.1, 51.2, 50.5 K/W, respectively. Likewise, the  $\eta_w$  was 58.6%, 54.1%, and 52.7%. In the second part, the heat-dissipation factor, optical power, luminous flux, and spectral flux of LP LEDs were estimated by extending the application of the equations that were employed for high-power (HP) LEDs. It was found there was a relative error of less than 15% between calculated and practical values. In the third part, the performance of thin film gallium nitride (ThinGaN) HP LED attached to a SinkPAD via solder was evaluated. Three types of solder: no-clean SAC305 (SP1), water-washable SAC305

(SP2), and no-clean Sn42/Bi57.6/Ag0.4 (SP3) were utilized. Findings revealed that  $R_{thja}$  for SP1, SP2, and SP3 was 5.76, 6.09, and 6.65 K/W. In the same way, at 1200 mA, the output power was 1330, 1288, and 1279 mW, respectively. Further, for current range 400-1200 mA, correlated color temperature (CCT) shift was 350, 406, and 768 K, respectively. The voids' effect of SP2 on the LED performance was assessed. The analysis showed that  $R_{thja}$  was 6.29, 5.79, 6.09, 6.39, and 7.71 K/W for LEDs 1-5. Furthermore, at 1200 mA and 80 °C, the luminous flux was 371.5, 367.8, 373.0, 360.3, and 351.7 lm, respectively. Moreover, the change in CCT was 755, 831, 1046.5, 1019, and 1779 K for the LEDs from 1 to 5. The LED thermal dynamic performance was analyzed using a multi-exponential function model. It was shown that the time constant of the LED package was on the order of 22 to 94 ms.

# CHAPTER 1

## INTRODUCTION

### 1.1 Solid-State Lighting (SSL) Technology Challenges

The lighting industry is presently undergoing a considerable transformation due to the proliferation of solid-state lighting (SSL) technology [1]. The quality and reliability of SSL technology have witnessed significant changes in the recent times. Hence, new materials and techniques are introduced, which will provide new classes of failure modes [2]. The SSL industry chain of LED comprises three classifications: upstream which consists of epitaxy growth, chip design and manufacturing; midstream, which denotes packaging; and downstream, which involves the lighting applications, as shown in Figure 1.1. The efficiency, light quality, and reliability of the LED product are interconnected with each aspect in the SSL industry chain [3].

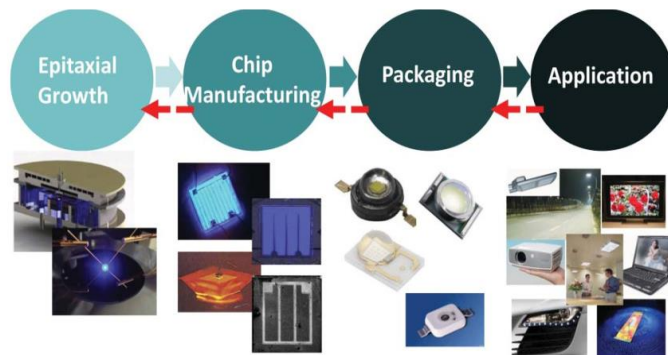


Figure 1.1 LED industry chain of manufacturing [3]

The reliability of the LED device is analyzed at different levels from 0 to 5. Level 0 denotes bare die, level 1 represents the LED package, level 2 is related to LED on board, level 3 is known as module which is LED and driver/optics/thermal, level 4 is related to luminaire, and level 5 is referred to as lighting system [2, 4] as presented in Figure 1.2. The reliability levels are related and interconnected with each other. Each level has its specific recognized failure modes that affect other failure modes. To

avoid failures and attain fast resolution of LED structural problems, an in-depth knowledge of the failure mechanisms and appropriate analytical techniques are required [5].



Figure 1.2 LED-based lighting system levels

## 1.2 Light-Emitting Diode Package

Light-emitting diodes are solid-state semiconductor devices that emit light at a specific wavelength. The color emitted from the LED is associated with the energy bandgap of the active layer material [6]. The key benefits of LEDs over conventional light sources are their small size, narrow spectrum, lengthy lifecycle, eco-friendliness, and low energy consumption [7-9]. The LEDs are extensively utilized in a number of applications that include signaling, signals display, liquid-crystal display (LCD) backlights, traffic lights, automotive, indicators, and general lighting [10-12]. Although LEDs are known as an efficient light source, approximately 60 to 70% significant amount of the input electrical power is converted to heat [13]. The LED package comprises a tiny semiconductor chip that is encapsulated in a silicone enclosure. The package shields the chip and offers optical, thermal, and electrical pathways. The major components of a typical lead frame LED package and their corresponding functions are shown in Figure 1.3. The solder joint is utilized to fuse the chip to the copper heat slug, which in turn causes the heat dissipation. The lead

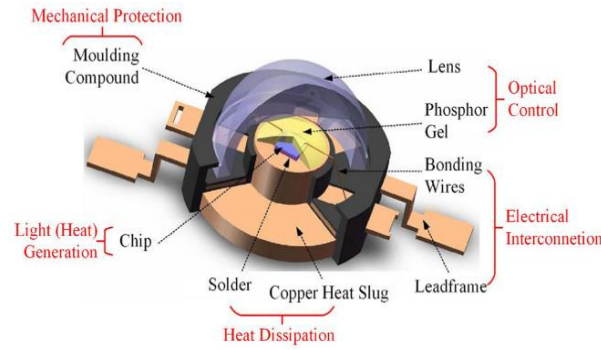


Figure 1.3 Typical lead frame LED package structure and parts functions [14]

frames and wire bonds are used for electrical connections, while the lens and phosphor are used to enhance light output and light conversion, respectively. The molding compound is utilized to maintain the heat slug and lead frames and to attach the lens. The light is extracted and disseminated through the lens while the heat is dissipated via convection and conduction through the heat slug to the ambient environment [14]. Packaging designs have been developed for three LED groups: (1) high-power (HP) LEDs which function at power level that exceeds 1 W; (2) medium-power (MP) LEDs which perform at power range of 0.25-1 W; and (3) low-power (LP) LEDs which perform at power level below 0.25 W [15].

### 1.3 LED Thermal Management

Viable thermal management implies the capacity to remove the heat and subsequently lessen the  $R_{th}$ . Thus, the relations between the LED parameters such as current, forward voltage, temperature, dissipated power, and light output must be taken into consideration. The LED's light output is dependent on forward current, temperature, and forward voltage. The LEDs thermal management can be either internal or external. The handling of thermal resistance ( $R_{th}$ ) from junction to the LED solder point is associated with the internal thermal management and must be performed throughout the manufacturing process. Nonetheless, the handling of the  $R_{th}$  from the

LED solder point to the ambience is linked to the external thermal management that comprises a selection of cooling mode, heat sink design, thermal interface materials, and bonding process [11]. The strategy to enhancing the external thermal management and efficient heat transfer entails the use of substrate and thermal interface material with good properties. Besides, larger interest must be provided to the thermal design issues even for low power lighting applications. For instance, efficient heat flow path is required to dissipate the heat from the LED to the system application for the  $R_{th}$  of 240-275 K/W [16].

The parameters that contribute to the increase in junction temperature ( $T_j$ ) include input current ( $I_f$ ), ambient temperature ( $T_a$ ), and thermal flow path. A Higher current increases the light output but leads to a drop in optical efficiency [17, 18]. The mechanisms that result from injection current and lead to efficiency droop include Auger recombination, carrier leakage, carrier delocalization, and electron overflow. Therefore, the efficiency droop is a result of the simultaneous action of junction temperature and current [19]. At constant current, the  $T_j$  has a linear proportionality with  $T_a$  [20]. The lower  $T_a$  initiates a significant temperature gradient, which then increases the heat dissipation efficiency. Since the LEDs operate at a moderate temperature, the generated heat is transferred mainly through conduction and convection. Although radiation still plays an important role, in LED lighting it is not the dominant heat transfer mechanism [21]. Besides, the temperature of the LED chip must be maintained below 120 °C, thus the heat dissipation of LED packaging through radiation could be neglected due to relatively low temperature [14, 22]. In addition, the LEDs' thermal management is often accomplished by the conduction due to multiple parts in the LED system and the heat energy must move across interfaces between parts [21]. The thermal path of the LED system comprises the LED device as

the light source, board, and external heat sink. Suitable thermal conduction path from die to ambient initiates a lower  $T_j$ . Thus, the thermal management has been transformed into a significant parameter for designing the LED device and system [23].

#### **1.4 Problem Statement**

Several essential problems are addressed in this study and highlighted as follows:

In recent times, LEDs have evolved into the ideal device in illumination. Thermal management design based on heat transfer theory is the bottleneck of LED technology applications and the thermal resistance is an evaluating factor [22, 24]. Thermal management is challenging due to the requirement for a lower junction temperature, which is related to both the chip design and packaging design [21]. Since a low operating temperature of the LED chip is very important, thermal management is strongly required for LED packaging and application products [22]. In practice, the internal thermal resistance of the LED depends on the geometry, die-attach material and chip size, while the external thermal resistance is influenced by the heat flow from the internal heat spreader of the LED to the surrounding environment [2]. The factors that affect the thermal conduction and external thermal resistance include a substrate, TIM, and defects on the solder layer. Given the ongoing miniaturization in optoelectronics, surface mounted device (SMD) LEDs have become relevant in advanced lighting. Thus, they have given more attention to research and development. SMD LEDs are widely used in mobile phones, laptops, hand-held products, and automotive applications [25]. This study is mainly focused on the evaluation of the



SMD LED performance with an emphasis on external thermal management using the heat conduction mode.

Despite the intensive research on the evaluation of LEDs, the assessments of the performance of InGaAlP low-power (LP) and ThinGaN high-power (HP) SMD LEDs remain limited. LP SMD LEDs have garnered interest in certain applications such as automotive and signaling due to their low heat production, long lifespan, and capability to generate saturated color with high efficiency. LP LEDs thermal resistance is very high (300 K/W [26, 27]) because of the lack of heat spreader that results in poor heat dissipation and subsequently affects the LED lifespan. The heat dissipation complexity of the LP LED remains unresolved. Therefore, this work is an attempt to improve the heat dissipation of InGaAlP LP LED using the substrate and a novel packaging structure to reduce the solder interface thermal resistance. To evaluate the thermal resistance, the heat conduction mode is used because the implementation of base structure provides a thermal path by conduction from the LED chip to the substrate [21]. A one-dimensional heat conduction path via Fourier's law and the structure functions reflect structural variations of the LED system.

To provide an optimum design for LP LEDs, a theoretical framework to estimate the parameters such as wall-plug efficiency ( $\eta_w$ ), heat-dissipation factor ( $k_h$ ), optical power ( $P_{opt}$ ), luminous flux ( $\varphi_v$ ), and spectral radiant flux ( $\Phi_v$ ) is important. In this study, same parameters for LP LEDs are estimated by extending the application of photo-electro-thermal (PET) theory equations [28-30] and spectrum model [31] that have been used for HP LEDs

Mounting LED on the substrate via the solder introduces a heat source into the illumination system. The solder layer between the LED device and the substrate is considered as a second level interconnection [32]. Moreover, the voids in the solder

layer cause an increase in thermal resistance [33] due to the reduction of the heat transfer effective area. In spite of some success has been achieved in the influence of the die attach layer and voids on heat flow from junction to the heat spreader [33-39], however, there is a lack of available information on the effect of solder and voids on the performance of HP SMD LEDs. Furthermore, the thermal time constant is a critical parameter that plays an important role in the optimal design of LEDs. Investigations on the dynamic thermal analysis have been carried out using analytical solutions or simulations to analyze the time constant of the chip, die-attach, submount and heat sink [40-43]. The study of the time constant of the LED package provides valuable information on the dynamic thermal performance and thermal structure of the device.

### **1.5 Objectives of Research**

This study is mainly focused on external thermal management of LP and HP SMD LED packages with an emphasis on the heat conduction mode. The objectives of this research include:

- i. To improve the thermal and optical performance of InGaAlP LP LED package using different substrates with and without embedding thermal interface material.
- ii. To analyze the heat-dissipation factor, optical power, luminous flux, and spectral radiant flux of InGaAlP LP LED package as a function electrical power and ambient temperature.
- iii. To investigate the influence of solder layer type and voids on thermal and optical performance of ThinGaN HP LED package.
- iv. To analyze and quantify the thermal time constant of ThinGaN HP LED package using the multi-exponential function model.

## 1.6 Thesis Outline

**Chapter 1** outlines the challenges in SSL technology and thermal management as well as the main limitations of LED lighting applications. In addition, the problem statement and objectives of the research are presented in this chapter. **Chapter 2** provides a concise review of the theory of heat transfer via conduction, the operating principle of LED device. The thermal and optical characterizations of the LEDs are also highlighted in this chapter. Furthermore, the substrates, thermally conductive materials, solders, and voids that contribute to LED thermal management are discussed in this chapter in detail. This chapter also covers the theoretical background of thermal transient measurement and characterization of the LED packages. In addition, the theories of heat dissipation factor, optical power, luminous flux, and spectral radiant flux estimations were comprehensively discussed in this chapter. **Chapter 3** deals with the experimental procedures employed to achieve the research goals. The experimental setup for the measurements is presented and explained in this chapter. The descriptions of the samples and instruments used in this work are also presented in this chapter. **Chapter 4** comprises the results and discussion of the performance of InGaAlP LP LED and ThinGaN HP LED. The effects of substrates and TIMs on the performance of the LED were discussed with the support of structure functions. In addition, the assessment of the heat dissipation factor, optical power, luminous flux, and spectral radiant flux was elaborated in this chapter. Furthermore, the impact of solder and voids on the performance of ThinGaN HP LED was discussed. This chapter also deliberates on the use of the multi-exponential model to analyse the thermal transient response curves of ThinGaN HP LED with different package designs. **Chapter 5** concludes the outcomes of this study, in addition to providing recommendations for future work.

## **CHAPTER 2**

### **LITERATURE REVIEW**

#### **2.1 Introduction**

This chapter reviews the potentiality of LEDs as a viable source of illumination. The chapter also provides an overview of the LED materials and packaging. It describes the operational principles, thermal management, thermal and optical characterizations of the LEDs. It emphasizes on the traditional and novel LED technologies. A brief historical overview of semiconductor materials and LED technology is also included in this chapter, followed by discussions on a wide array of LED packages. In addition, this chapter presents a theoretical background of the assessed parameters for InGaAlP LP SMD LEDs.

#### **2.2 Conduction Heat Transfer Theory**

The generated heat at the chip must be dissipated from the LED to sustain a low junction temperature. Heat energy can be transferred through different mechanisms from one layer to another in the form of a heat flow. Heat transfer frequently occurs where a temperature difference exists between the two objects. The heat diffuses from the high temperature object to the one of low temperature. Heat is basically transferred via conduction, convection, and radiation. Thermal conduction results from the interactions between the atoms and particles. In the collision of contiguous or adjoining molecules, the transfer of energy from more energetic to less energetic molecules must arise towards the direction of declining temperature as illustrated in Figure 2.1.

The conduction in solids may be credited to the atomic activity in the form of lattice vibrations [44] as presented in Figure 2.2. At the molecular level, the intrinsic heat energy of a higher energy level molecule is first converted to vibrating kinetic

energy, which is then transferred to adjoining atoms. This process is reiterated till the temperature gradient between two adjoining atoms reaches zero (equilibrium state).

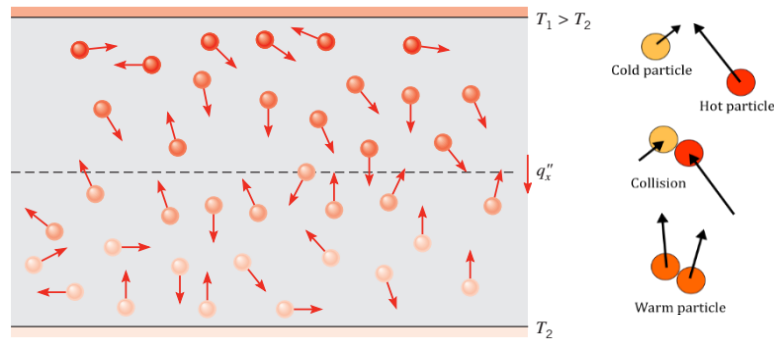


Figure 2.1 Thermal conduction with energy diffusion due to molecular activities [44] and particle collisions

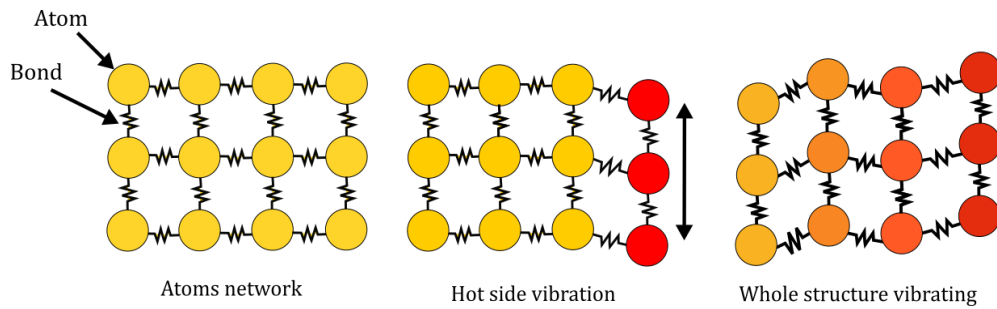


Figure 2.2 Thermal conduction by lattice vibrations [45]

As observed in Figure 2.3, the transfer of heat via one-dimensional (1D) thermal conduction is explained by Fourier's law and mathematically expressed as [44, 46]:

$$q_x = -k_{th} \cdot A \cdot \frac{dT}{dx} \quad (2.1)$$

where  $q_x$ ,  $A$ ,  $k_{th}$  and  $dT/dx$  denote heat transfer rate in x-direction, area normal to the

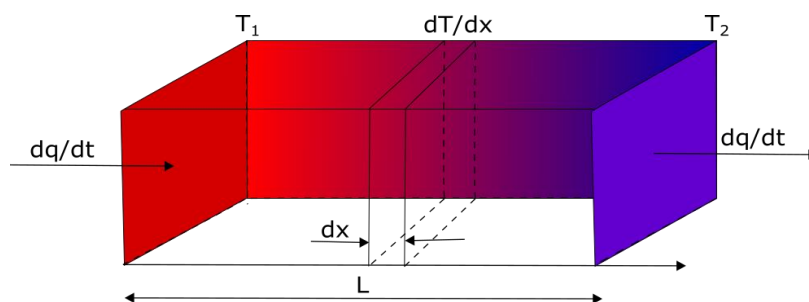


Figure 2.3 One-dimensional thermal conduction analysis [47]

heat flow path, material thermal conductivity, and temperature gradient along the x-direction, respectively. In the case of steady-state conditions with linear temperature distribution, the temperature gradient may be expressed as:

$$\frac{dT}{dx} = \frac{T_2 - T_1}{L} \quad (2.2)$$

Thus, the heat flux is specified as [44, 48]:

$$q_x'' = -k_{th} \frac{T_2 - T_1}{L} = k_{th} \frac{\Delta T}{L} \quad (2.3)$$

where  $q_x''$  is the heat flux ( $W/m^2$ ) which means the heat transfer rate per unit area perpendicular to the direction of heat flow. For 1D heat transfer with no internally generated energy and constant properties, a major theory is suggested through Eq. 2.3. The relationship between thermal resistance and heat conduction parallels that of electrical resistance and electrical conduction. Using Eq. 2.3, the thermal resistance for conduction in a plane wall is expressed as follows:

$$R_{th} = \frac{T_1 - T_2}{q_x} = \frac{L}{k_{th} \cdot A} \quad (2.4)$$

Since the LEDs are operated at much more moderate temperature, the generated heat at the chip is mainly transferred via conduction and convection [49]. The LED's thermal management is often accomplished by the conduction due to multiple parts of the LED system and the heat energy must move across interfaces between parts [21]. Therefore, the primary heat transfer mode inside the component or package is the conduction [50] and a successful design should have low thermal resistance between the junction and the heat sink [23]. This research focused on the heat conduction path with the aid of structure functions and one-dimensional Fourier's law of heat conduction to get the thermal resistance and junction temperature.

### 2.3 Light-Emitting Diodes

The LED is a semiconductor device that has the ability to convert electrical energy into light. The structure of energy band ( $E_g$ ) of semiconductor material is an important parameter that figures out the properties of the emitted light. There are two types of semiconductor materials: direct bandgap and indirect bandgap material. In direct bandgap material, the top of the valence band (VB) and the bottom of the conduction band (CB) are at the same value of momentum (Figure 2.4(a)). However, in indirect bandgap material, the top of the VB occurs at a dissimilar value of momentum to the bottom of the CB energy (Figure 2.4(b)). In direct bandgap semiconductor, the electron can directly emit a photon, however, in indirect bandgap semiconductor, a photon is not emitted directly because the electron must cross a transitional state. The light efficiency from the LED depends on the electron-hole (e-h) recombination in the semiconductor of the direct bandgap. Thus, the recombination of the electron and hole in indirect bandgap semiconductor entails phonons (heat). Some unconfined photons may be reabsorbed into the semiconductor material and generate the e-h pair afterwards, whereas other emitted photons will be reflected due to total internal reflection, contacts, and surface interface of semiconductor. The light extraction can be amplified by utilizing a chip design, and modification of the surface structure and fabrication [51].

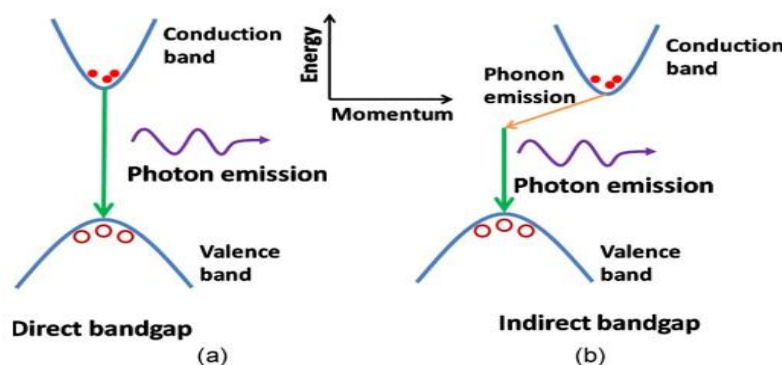


Figure 2.4 Process of photon emission in (a) direct bandgap and (b) indirect bandgap semiconductors [52]

Homojunction LED is the most basic diode structure as illustrated in Figure 2.5(a). In this LED, both the p- and n-type are intrinsic materials with similar  $E_g$ , but created from different dopant materials. As the current flows through, the VB is partly

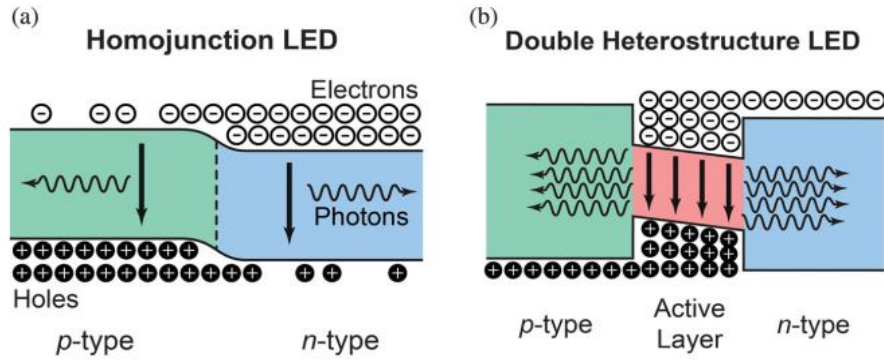


Figure 2.5 Schematic diagram of energy band for (a) homojunction LED and (b) double-heterostructure LED [53]

emptied, and CB is incompletely filled, without recombination decay at the diode junction. This process is referred to as current diffusion. Furthermore, a depletion region is generated at the p-n junction when the forward voltage ( $V_f$ ) is zero. The potential difference at p-n junction impedes more e-h recombination, which results in the decline of the LED efficiency. Heterojunction LEDs are fabricated to enhance the carrier confinement, which increases the e-h recombination and constrain the diffusion current and photons reabsorption. In the heterojunction LED, a semiconductor of narrow  $E_g$  is flanked by two materials with a wide  $E_g$ . In this case, the free holes and electrons are confined into the barriers or quantum well (QW) during the  $V_f$  operation, thus increasing the probability of e-h recombination and increasing the efficiency of the LED. The currently used LEDs were transformed into an alternative structure to acquire more effective light and significant carrier concentrations. This structure is a double heterostructure (DH) that is composed of the active region and two confinement layers that clad the active region. Thus, there exist two junctions that are derived from three



parts in the diode as displayed in Figure 2.5(b). This structure induces agglomeration of the charge carriers in the active region instead of diffusing through the diode, which is followed by recombination of the charge carriers in the active region and subsequent production of photons with energy close to the active layer  $E_g$ . In recent times, HP LEDs are made with high external quantum efficiency (EQE) that is attributable to increase in QWs number. The preferred light colors can be modified by choosing the appropriate semiconductor of a specified  $E_g$ . InGaN/GaN is extensively utilized to manufacture green to blue LEDs, while InGaAlP compounds are used for the production of red to yellow LEDs [54, 55]. White LEDs are fabricated via the combination of red-green-blue (RGB) emitters. White light can also be achieved by creating a phosphor layer over the blue LED chips. Highly efficient white LEDs can be produced via the excitation of cerium-doped yttrium aluminum garnet (YAG: Ce) yellow phosphor by the blue light [56-59]. The spectrum, concentration, and thickness of the phosphor can be adjusted to fit the color in cool white, warm white or in between [60]. In addition, the red, green, blue, or yellow phosphors can be exploited with ultraviolet (UV) LEDs to generate white light [61].

## **2.4 LED Operation Principle**

The fundamental structure of the LED is illustrated in Figure 2.6. In the case of DH LED, the active region  $E_g$  is smaller compared to those of p-type and n-type semiconductor. With the application of a forward bias by means of an external current source, the electrons and holes are sourced from the n-type and p-type, respectively, into the active region. The photons are subsequently emitted when electrons and holes recombine radiatively. As the electron reaches the hole, it drops across the bandgap from higher energy level to lower energy level, thus leaving the bandgap in the form of

photon with a specific wavelength. The peak wavelength ( $\lambda_p$ ) of the emitted photon is derived from the  $E_g$  as follows [23, 54, 62]:

$$E_g (ev) = \frac{1240}{\lambda_p (nm)} \quad (2.5)$$

For instance, increasing the level of impurities will decrease the  $E_g$ , thus increasing the wavelength of the emitted photon.

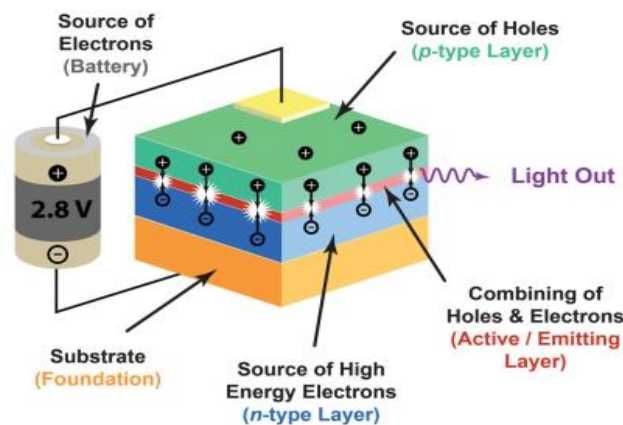


Figure 2.6 Schematic sketch of double-heterostructure LED and a battery for operating the LED [53]

The QWs are constructed in the active layer to enhance the efficiency of LEDs. The QWs are composed of very thin layer (few nm) which is fabricated from a lower  $E_g$  material. The color of the light can be differentiated by controlling the composition and the thickness of the QW. The multi QWs (MQWs) comprises both wide and narrow  $E_g$  materials. The working mechanism of LED entails the injection of the electrons and holes into the MQWs and their subsequent recombination to generate photons or heat. The recombination of electrons and holes can be either radiative or non-radiative. The photons result from the radiative recombination, which is the crucial objective of using LEDs. On the other hand, non-radiative recombination is due to the vibration of carrier-lattice or interaction between carrier and phonon. In addition, the non-radiative recombination includes Auger recombination and defects which produce heat.

## 2.5 Overview on LED Packaging

Improving the growth technology of SSL is critical to enhancing the design of the LED package. The heat produced at junction should be extracted which can be achieved by decreasing the  $R_{th}$  of the LED package. New LED packages have been developed for automotive head lighting applications, which are functional at input power that exceeds 15 W and emit white light with luminous flux close to 1000 lm [63].

### 2.5.1 Packaging of Low-Power LED

The LEDs utilized in a number of lighting and LCD backlighting applications are LP or MP LEDs [15]. The LP LED package refers to the epoxy resin, which was originally invented for LP indoor applications. This LED has a high thermal resistance and electrical power confined to a few 100s of mW. A novel kind of LP LED package is the surface mount device (SMD). There are numerous benefits associated with the use of SMD for industrial production, which include faster setting in automatic devices, less parasitic effects, minute dimensions, and cost effectiveness. An archetypal LP SMD LED package is displayed in Figure 2.7. Here, the chip is fused to the lead frame which has a plastic molding housing. The top electrode of the chip is linked to the other half of lead frame using a wire bond. Finally, the housing is packed with encapsulation resin. These packages have miniature size range of 0.5-1 mm, which is higher than that of die.

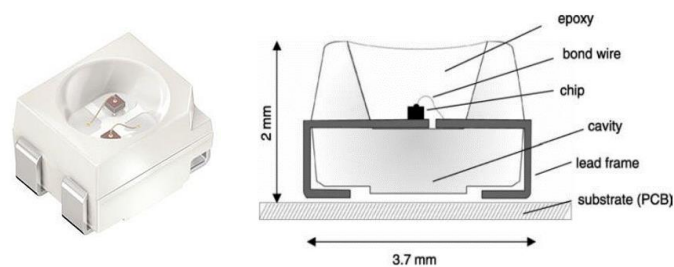


Figure 2.7 An example of Osram LP SMD LED package (TOPLED) and its schematic diagram [64]

The maximum forward current of LP SMD LED packages is constrained to 100-150 mA, which is attributable to their higher total  $R_{th}$  that ranges from 300 to 500 K/W.

InGaAlP-based LP SMD LEDs are evolving into the preferred material as a result of their high efficiency and long wavelength visible spectrum [65]. The benefits of InGaAlP LP LEDs include low operational settings, lower heat production, and ability to generate saturated colors with high luminous efficacy. They are extensively utilized in several applications, such as automotive lighting, traffic signals, indicators, and color displays at different ambient temperatures [66-68]. In contrast to HP LEDs,  $R_{th}$  and  $T_j$  of LP SMD LED is significantly more affected by  $T_a$  than  $I_f$ .

### **2.5.2 Packaging of High-Power LED**

HP LEDs are fabricated to be operated at 1.0 A or a more forward current. The energy dissipation in this LED package is above 1.0 W. This LED package comprises a die with area that exceeds 1 mm<sup>2</sup>. Despite the various kinds of HP LED packages, SMD package is largely selected because it is fitting for the heat dissipation. HP LEDs with SMD packages are one of the vital products of most LED manufacturing companies. There are two categories of the structure of HP SMD packages, as shown in Figure 2.8. The first is the LED chip affixed to the heat slug of Cu or Al material. Since the heat slug is characterized by high thermal conductivity, this LED has low  $R_{th}$ . Examples of LED packages with heat slug include Dragon-series of Osram Opto Semiconductors and LUXEON K2-series of Philips Lumileds. The second type of HP SMD LEDs utilizes ceramic (AlN, AlO<sub>x</sub>, etc.) as a dielectric material, where the LED thermal pad is electrically insulated and electrical vias are used to link the anode and cathode. It is a less complex process to arrange ceramic packages into arrays, and thermal vias can be applied at the bottom of LED thermal pad.

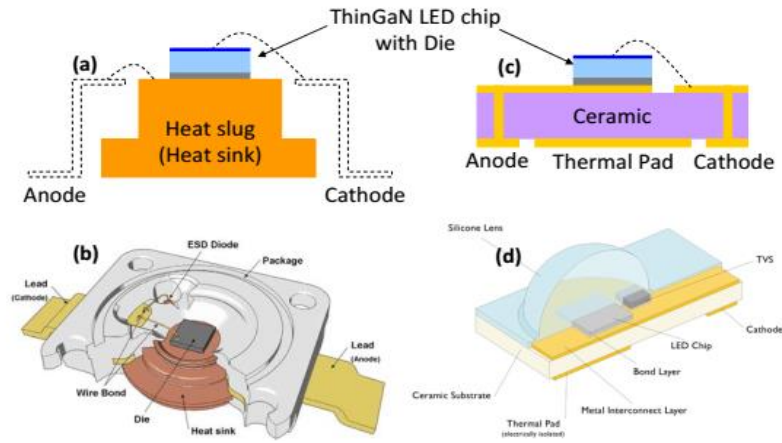


Figure 2.8 HP LEDs with SMD packages: (a) LED chip attached to heat slug, (b) structure of Osram Dragon series LED, (c) LED chip attached to a ceramic substrate, and (d) structure of LUXEON Rebel of Philips Lumileds [69]

## 2.6 LED Thermal Characteristics

It is anticipated that the LED lighting will be extensively used in the illumination markets in near future by ensuring the maximum light conversion efficiency. However, a part of the electrical input power is expelled as heat which is the principal weakness of the LED. Hence, some thermal properties of the LED devices should be considered.

### 2.6.1 Heat Transfer Mechanism in LED Package

There are three mechanisms of heat transfer: conduction, convection, and radiation. The heat generated at junction is conducted through the bottom side of chip to the ambient environment via a long thermal path, which extends from the junction to solder point, solder point to a board, and board to the heat sink and lastly to the environment. To reduce the  $T_j$ , each  $R_{th}$  in the thermal path must be minimized. One area of interest in thermal packaging is advances in TIMs, used to join two materials in the overall heat flow path. A key focus is on improved TIMs, used in joining surfaces in a microelectronic package to reduce interface thermal resistance [70]. The commonly known TIMs include epoxy, thermal grease, adhesive, and solder. The heat dissipates

through substrate and heat sink via conduction and convection. The package design, surface roughness, type and quality of each component, type and thickness of TIM, and contact area are the critical parameters of the design of  $R_{th}$ .

## 2.6.2 Thermal Measurements of LEDs

The thermal transient measurement of the LED is presented in Figure 2.9. It is apparent that the electrical input power ( $P_{el}$ ) is transformed into light and heat. The heat can be established in the course of the thermal transient testing. At low current, the

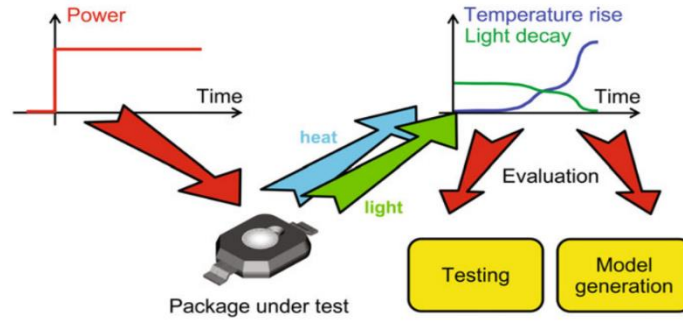


Figure 2.9 Thermal transient measurement of LED package [21]

relationship between the change in junction temperature ( $\Delta T_j$ ) and the change forward voltage of the p-n junction ( $\Delta V_f$ ) is a linear and the slope of this relation is a temperature-sensitive parameter (TSP):

$$\text{TSP} = \frac{1}{\text{K}} = \frac{\Delta V_f}{\Delta T_j} \quad (2.6)$$

The LED thermal resistance from junction to the ambient ( $R_{thja}$ ) is defined as:

$$R_{thja} = \frac{\Delta T_j}{\Delta P_{el}} = \frac{\Delta V_f}{\text{TSP} \cdot \Delta P_{el}} = K \cdot \frac{\Delta V_f}{(P_{el1} - P_{el2})} \quad (2.7)$$

The  $V_f$  method is used to measure the thermal characteristics of the LED and is referred to as transient response measurement. Figure 2.10(a) shows the temperature dependence of  $V_f$  when a continuous small current ( $I_M$ ) is applied across the junction. The electrical

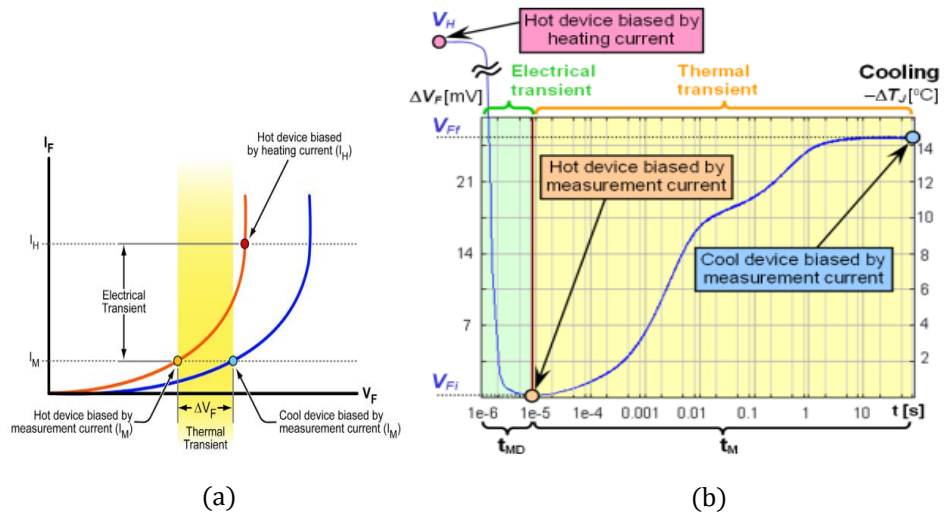


Figure 2.10 (a) Heating followed by cooling cycle [71] and (b) actual transient of a diode that scaled in voltage and temperature [21]

transient unavoidably occurs due to a sudden switching of the current. This transient consumes very minute time ( $\sim 10\mu\text{s}$ ) where the change in  $V_f$  does not simultaneously result in a temperature change. After resolving the electrical transient, the thermal transient can be obtained as presented in Figure 2.10(b). The principle of the measurement is recommended by Joint Electron Device Engineering Council (JEDEC) Standard JESD51-1 [72] and JESD51-51 [73]. The heating or cooling curve is derived by converting the current from high heating current ( $I_H$ ) to low sensor current ( $I_S$ ).

### 2.6.3 Structure Functions

It is important to assess the factors that contribute to the rise in thermal resistance in the conductive path. The structure function is a plot of the cumulative thermal resistance ( $R_{th\Sigma}$ ) versus the cumulative thermal capacitance ( $C_{th\Sigma}$ ) along the heat path [74]. A few microseconds are required to increase the temperature after excitation, however 100s or 1000s of seconds are prerequisite to attain the steady state. Therefore, transient response functions are typically planned on a logarithmic time scale [75]. According to JEDEC JESD51 series, sensor current ( $I_S$ ), which is referred to as

measured current ( $I_M$ ) and heating current ( $I_H$ ), is the summation of  $I_S$  and drive current ( $I_D$ ). The switching from  $I_H$  to  $I_S$  happens a single time. During heating, both  $I_D$  and  $I_S$  are implemented on the LED. After the device reaches steady state,  $I_D$  is turned off and the transient cooling curve is only derived under  $I_S$  as shown in Figure 2.11. Based on thermal and electrical parallels, thermal resistance, and thermal capacitance of packaged components can be articulated. RC network is denoted in two forms: Foster with chain model and Cauer network with ladder model as presented in Figure 2.12 [76]. The transformation of Foster network into Cauer equivalent is crucial for identifying the heat-flow path. The equivalent circuit is Cauer network which is appropriate to solve the heat flow problems, since heat is ultimately flowing to the ambience [40].

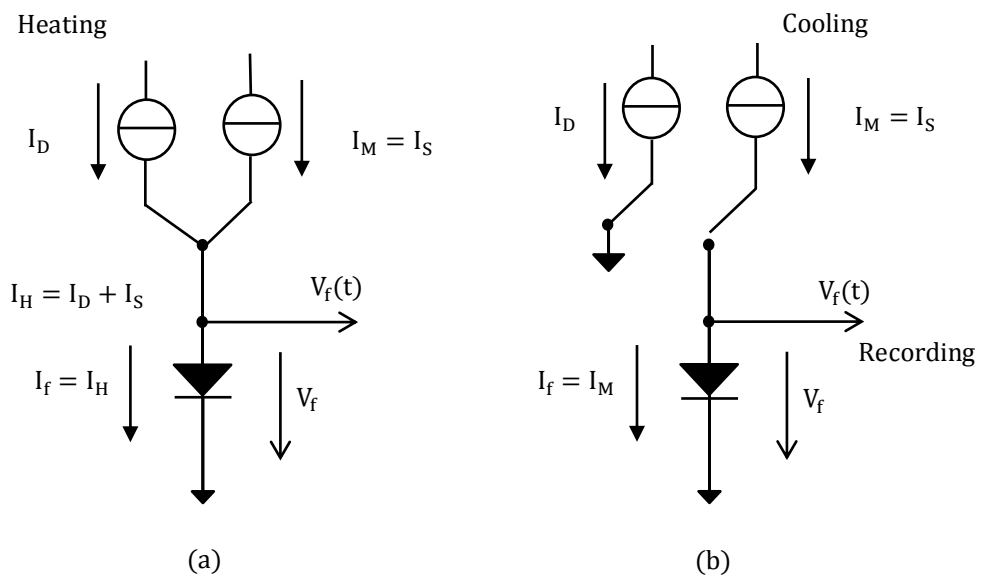


Figure 2.11 Practical comprehension of the diode measurement scheme at applying: (a) heating current and (b) measured current [21]

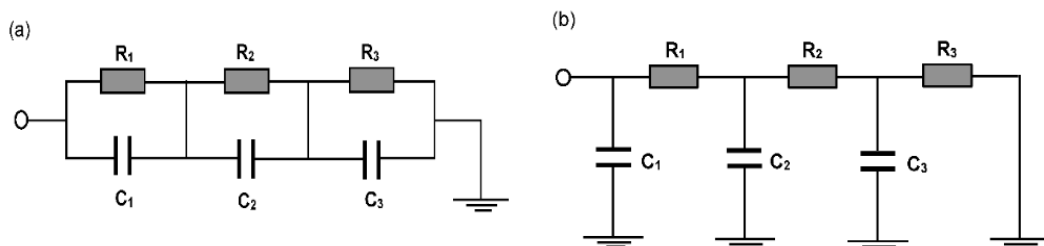


Figure 2.12 (a) Foster network and (b) Cauer network [76]



Structure functions are utilized to explore the modifications in a material and cross-sectional area in the heat-flow path. The partial  $R_{th}$  can be derived from the horizontal axis of the structure functions curve. A cumulative structure function is defined as the  $C_{th\Sigma}$  with regard to the  $R_{th\Sigma}$ . In the cumulative structure function curve, the material with higher  $R_{th}$  value is represented by plateau; however, the material with lower  $R_{th}$  is represented by steep region [77, 78]. The  $R_{th}$ ,  $C_{th}$ , and material dimensions can be directly read from the cumulative structure functions. Differential structure functions are the derivative of  $C_{th\Sigma}$  with respect to  $R_{th\Sigma}$  as [77, 79]:

$$K_{th}(R_{th\Sigma}) = \frac{dC_{th\Sigma}}{dR_{th\Sigma}} = c_V \cdot k_{th} \cdot A^2 \quad (2.8)$$

where  $c_V$  is the volumetric heat capacitance ( $J/m^3.K$ ),  $A$  is the cross-sectional area at position along heat flow path ( $m^2$ ), and  $k_{th}$  is the thermal conductivity ( $W/m.K$ ). It is occasionally less difficult to differentiate the interface between sections by means of differential structure functions. Here, the peak specifies a material with high  $k_{th}$  such as chip or heat sink, and valley denotes a low  $k_{th}$  material such as air. The inflection points between peaks and valleys signify interface regions.

#### 2.6.4 Junction Temperature, $T_j$

The  $T_j$  is a critical factor that affects the quantum efficiency, output power, lifetime, and reliability of the LED device [80-84]. High  $T_j$  will initiate a non-radiative recombination of carriers and decrease the efficiency of emitted light [85]. Therefore, the low and stabilized  $T_j$  is essential in the course of LED operation. When the LED is energized at high current, there is a surge in the heat produced at the LED chip. The series resistance ( $R_s$ ) decreases at high temperature due to the higher activation of the acceptor atoms and high  $k_{th}$  of both active region and p-type layer [86]. The  $T_j$  of most

commercial LEDs must not surpass specified value e.g. 125 °C that is recognized in the LED datasheet and dependent on the LED model. The maximum  $T_j$  should be averted as surpassing this value may lead to the package failure [87].

### 2.6.5 Thermal Resistance, $R_{th}$

The  $R_{th}$  of a semiconductor device is a measure of the ability to dissipate the heat generated and expressed in K/W or °C/W. The electrical  $R_{th}$  ( $R_{th,el}$ ) is defined without including the heat dissipation power ( $P_{heat}$ ), while the real  $R_{th}$  ( $R_{th,real}$ ) is considered the  $P_{heat}$  [88, 89]. The  $R_{th,el}$  is the ratio of  $\Delta T_j$  and ( $P_{el}$ ) and given as:

$$R_{th,el} = \frac{\Delta T_j}{P_{el}} = \frac{T_j - T_a}{I_f \times V_f} \quad (2.9)$$

The  $R_{th,real}$  is defined as:

$$R_{th,real} = \frac{\Delta T_j}{P_{heat}} = \frac{T_j - T_a}{P_{el} - P_{opt}} \quad (2.10)$$

The  $R_{th}$  from LED junction to ambience ( $R_{thja}$ ) is called total thermal resistance. Also, the  $R_{th}$  from LED junction to solder point ( $R_{thjs}$ ) is known as LED package  $R_{th}$  and usually provided in datasheets of LED's manufacturers.  $R_{thjs}$  is a significant parameter that helps to understand the limit of LED thermal performance when the LED is attached to a suitable board or heatsink. For system that involves conduction between various materials and surfaces, a simple model of thermal path is a series  $R_{th}$  network that is identical to the electrical circuit. The  $R_{th}$  is represented by the resistor, the flow of heat is identified by the electrical current, and the electrical voltage is indicated the temperature of the LED device. The heat generated at the junction is first conducted through the LED components to the solder point. Then, through the layers of different  $R_{th}$  to the board and through the TIM to the heatsink and

finally through convection and radiation to the ambient [90]. The  $R_{thja}$  formula of the LED system is the sum of individual  $R_{th}$  in series which is from junction to solder point, solder point to board, board to heatsink, and from heatsink to the ambient.

### 2.6.6 Thermal Time Constant, $\tau_{th}$

Thermal time constant ( $\tau_{th}$ ) is a valuable factor since it provides information on dynamic thermal performance and device structure [40]. The  $\tau_{th}$  for heating or cooling process of 1D heat transfer structure can be computed as:

$$\tau_{th} = R_{th} C_{th} \quad (2.11)$$

Increasing the time for temperature rise provides the LED engineers an opportunity to recommend a technique for heat dissipation. The materials characterized by high  $C_{th}$  and low  $R_{th}$  are ideal for the extension of  $\tau_{th}$  of the LED package [43]. The  $\tau_{th}$  variation between LEDs is imputed to the design, material properties, geometric structure, thermal conductivity, specific heat of LED system structure [79].

The dynamic thermal behavior of LED devices can be examined using the Cauer network. After switching on the power, the transient thermal response can be expressed as the summation of distinct exponential functions as follows [40]:

$$\Delta T(t) = \sum_{i=1}^n \Delta T_i \left[ 1 - \exp\left(-\frac{t}{\tau_{thi}}\right) \right] \quad (2.12)$$

where  $\Delta T(t)$ ,  $t$ ,  $\Delta T_i$  and  $\tau_{thi}$  represent the junction temperature rise, applying time, temperature rise and thermal time constant of the  $i$ th layer, respectively. The number of layers is dependent on the design of the LED system [91]. Furthermore, it is imperative to use a logarithmic time scale that enables the identification of the separate layers of the LED system. Following the switching off of power, the transient thermal response can be formulated as a multi-exponential decay function [40]: